

# Nuclear Inelastic X-Ray Scattering of FeO to 48 GPa

Viktor V. Struzhkin, Ho-kwang Mao, Jingzhu Hu, Markus Schwoerer-Böhning, Jinfu Shu, and Russell J. Hemley  
*Geophysical Laboratory and Center for High Pressure Research, Carnegie Institution of Washington,  
5251 Broad Branch Road NW, Washington, DC 20015, USA, and  
HPCAT, Advanced Photon Source, Argonne National Laboratory, Argonne, IL 60439, USA*

Wolfgang Sturhahn, Michael Y. Hu, and Ercan E. Alp  
*Advanced Photon Source, Argonne National Laboratory, Argonne, IL 60439, USA*

Peter Eng and Guoyin Shen  
*University of Chicago, 5640 South Ellis, Chicago, IL 60637, USA, and GSECARS, Advanced Photon Source, Argonne  
National Laboratory, Argonne, IL 60439, USA*  
(April 26, 2024)

The partial density of vibrational states has been measured for Fe in compressed FeO (wüstite) using nuclear resonant inelastic x-ray scattering. Substantial changes have been observed in the overall shape of the density of states close to the magnetic transition around 20 GPa from the paramagnetic (low pressure) to the antiferromagnetic (high pressure) state. Our data indicate a substantial softening of the aggregate sound velocities far below the transition, starting between 5 and 10 GPa. This is consistent with recent radial x-ray diffraction measurements of the elastic constants in FeO. The results indicate that strong magnetoelastic coupling in FeO is the driving force behind the changes in the phonon spectrum of FeO.

The study of the electronic and magnetic properties of simple transition-metal compounds is an important topic in diverse fields ranging from solid-state physics to Earth sciences. Iron oxide FeO (wüstite) belongs to the group of highly correlated transition metal oxides, being an archetypal insulating antiferromagnetic material at zero temperature. NiO, CoO, MnO fall in the same group of materials, which are still not well understood by theory. They also present a challenge to experimentalists because the predicted high pressure transformations in these materials (metallization, high-spin to low-spin transitions) may occur at extreme pressures (e. g.  $> 100$  GPa). FeO stands out from this group of materials in the sense that it is a possible major constituent of the Earth's lower mantle and core, thus its pressure and temperature dependent properties are very important for the understanding of the Earth's interior. Here we present a study of the vibrational density of states of isotope-enriched  $\text{Fe}_{0.947}\text{O}$  using high-resolution nuclear resonant inelastic x-ray scattering. We observe changes in the density of states that are consistent with the softening of the aggregate shear sound wave velocity of wüstite under pressure [1], which we associate with the phase transition from the cubic paramagnetic phase to the rhombohedrally distorted antiferromagnetic phase stable at higher pressures. We show that the phonon density of states is affected by magnetoelastic coupling between phonon and spin subsystems in FeO.

Experiments were performed at the synchrotron beamline SRI-CAT 3ID of the Advanced Photon Source (APS), Argonne National Laboratory. The details of the

diamond cell and the experimental setup are reported elsewhere [2]. The sample was  $\sim 25 \mu\text{m}$  in diameter (loaded without pressure medium), and diamonds with flat  $400 \mu\text{m}$  culets were used. The maximum counting rate in the phonon wing ranged from 10 cps at 0.9 GPa to 2 cps at 48 GPa. The measured spectra, i. e., count rate as a function of the energy difference between the incident photon energy and the nuclear transition energy,  $I(\Delta E)$ , were converted to phonon DOS profile according to the data analysis procedure described by Hu et al. [3]. Typically, 10-20 DOS spectra (one hour/spectrum) at the same pressure were summed together. The pressure was measured using the ruby fluorescence line and a nonhydrostatic pressure scale [4].

Experimental data are presented in Fig.1. In Fig.2 we compare the phonon DOS of FeO as derived from neutron scattering [5] and the partial phonon DOS of Fe at 0.9 GPa from our measurements. High frequency oxygen modes are absent from our data, indicating that Fe vibrational amplitude is negligible at oxygen vibrational frequencies. One apparent feature of the experimental data is an inelastic peak at small energy transfers which develops at 10 GPa, and persists through almost the entire pressure range of the present experiment to 48 GPa. It is most pronounced near 16 and 20 GPa, which is exactly the pressure range of the reported transition from the paramagnetic rock-salt-type structure to the antiferromagnetic rhombohedral structure [6,7]. The transition is very sensitive to (nonhydrostatic) stress conditions [6]; for example, the splitting of the (111) diffraction line being smeared between 10 to 18 GPa if no pressure medium

was used, and occurring around 16 GPa [6] to 17 GPa [1] under quasihydrostatic conditions.

The calculated partial density of states weighted by the square of the energy  $E^2$  is plotted versus energy in Fig.3. In Fig.3, the density of states in the Debye approximation would be a straight horizontal line, related to the aggregate sound velocity of the material [2,8]. The apparent feature of our data is the pronounced softening of the low energy vibrational spectrum. The resolution of the present measurements (2.4 meV) does not allow us to follow the softening to the low frequency region, where most static and ultrasonic measurements are performed. However, this behavior suggests large effects on the static elastic constants at the Néel transition.

The temperature dependence of the elastic constants of  $\text{Fe}_{0.92}\text{O}$  at ambient pressure was investigated in detail by Sumino et al. [9]. Substantial softening of the shear constant  $C_{44}$  was found close to the Néel transition. Similar anomalies have also been observed in  $\text{MnO}$  (softening of  $C_{44}$ ) [11]. The magnetic structure studies [15–17] by neutron scattering have shown that the Mn spins align ferromagnetically within a given (111) plane, and these planes are stacked antiferromagnetically in the  $\langle 111 \rangle$  direction. Similarly,  $\text{FeO}$  has the same magnetic structure, with magnetic moments pointing in the  $\langle 111 \rangle$  direction. At temperatures below the Néel temperature  $\text{MnO}$  undergoes a lattice contraction along the antiferromagnetic stacking direction  $\langle 111 \rangle$  [18]. The distortion in  $\text{FeO}$  has different sign, the elongation along the body diagonal. The magnetic system breaks into multiple domains (called T domains) corresponding to the antiferromagnetic stacking along the four possible  $\langle 111 \rangle$  directions within the crystal. Experimental [18–20] and theoretical [21–23] studies in  $\text{MnO}$  invoke exchange-striction effects to explain the character of the transition. The results of these studies can be summarized as follows. The energy balance is determined by minimizing the sum of magnetic exchange energy and elastic energy, resulting in a rhombohedral distortion

$$\Delta = z_1 N J_1 \epsilon_1 S^2 / 24 C_{44} \quad (1)$$

Here  $\Delta$  denotes the distortion of trigonally deformed cube corner angles  $\frac{1}{2}\pi \pm \Delta$ ,  $C_{44}$  is the shear constant,  $J_1$  is the exchange integral for the nearest neighbors,  $z_1$  is the number of the nearest neighbors,  $\epsilon_1 = -r \delta \ln J_1 / \delta r$ , and  $S^2 = \langle S_i \cdot S_j \rangle_{nn}^p - \langle S_i \cdot S_j \rangle_{nn}^a$  is a correlation function for nearest neighbors with parallel spins (residing within the same  $\langle 111 \rangle$  plane) and antiparallel spins in neighboring  $\langle 111 \rangle$  planes. The numerical value of  $\Delta$  is about 0.5 degree at 4 K in  $\text{MnO}$ . Actually, according to Bartel, [22]  $\Delta$  is proportional to the sublattice magnetization and is a sensitive measure of the order parameter of the magnetic phase.

However,  $\text{FeO}$  and  $\text{CoO}$  have much larger volume anomalies below  $T_N$  and their magnetic properties according to Kanamori [24,25] cannot be described by the

theory developed by Lines and Bartel [22]. In a crystal field of cubic symmetry, the orbital degeneracies of  $\text{Fe}^{2+}$  and  $\text{Co}^{2+}$  are not completely removed, and the residual orbital angular momenta contribute to the energy balance through spin-orbit coupling and the direct effect of orbital magnetic moments, resulting in observable magnetostriction effects. Substantial contribution to the magnetostriction effects in  $\text{FeO}$  is due to the magnetic anisotropy energy [25]. Kanamori [25] calculated the equilibrium strain components for  $\text{FeO}$  resulting from magnetostriction. He used the general formulation derived by Kittel for cubic systems [26] (all  $C_{ij}$ 's are cubic elastic constants,  $B_1$  and  $B_2$  are cubic magnetoelastic constants):

$$\begin{aligned} e_{ii} &= B_1 ((1/3) - \alpha_i^2) / (C_{11} - C_{12}), \\ e_{ij} &= -B_2 \alpha_i \alpha_j / C_{44} \end{aligned} \quad (2)$$

where  $\alpha_i$  are direction cosines of the magnetization. Kanamori's treatment leads to an elongation along [111] diagonal in  $\text{FeO}$ , which agrees with experimental results [17]. From the experiments on  $\text{FeO}$  at 95 K [28] one derives a rhombohedral angle of  $59^\circ 32'$ , or  $e_{xy} = 0.705\%$ . To estimate the rhombohedral distortion resulting from the exchange interaction (Eq.1) in  $\text{FeO}$ , we need reliable information about the exchange integrals and their dependence on the lattice parameter, which to our knowledge is not available at the moment. The experimental values of distortion [1,6] seem to be quite close to the Kanamori's calculation. Moreover, rhombohedral distortion is enhanced at high pressures [6], indicating increasing  $B_2$  in  $\text{FeO}$  under pressure.

The cubic constant  $B_2$  is responsible for the magnetoelastic coupling between the phonon and the magnon branches, and our results on the enhanced phonon density of states are directly related to the magnetoelastic coupling in  $\text{FeO}$ . The expression for phonon dispersion including the magnetoelastic coupling follows from the equations of motion for the magnetic moment [29,30]:

$$(\omega^2 - \omega_m^2)(\omega^2 - \omega_s^2) - \frac{gk^2 B_2^2 \Omega}{2\rho M_0} = 0 \quad (3)$$

Here  $\omega_s$  is the frequency of sound wave, and  $\omega_m^2 = \Omega g M_0 (\beta + \alpha k^2)$  is the spin wave frequency in the absence of magnetoelastic coupling;  $\rho$  is the density of the material,  $M_0$  is the magnitude of the magnetic moment of one sublattice,  $\Omega = g M_0 (\beta + 2\gamma)$ . The parameters  $\alpha$ ,  $\gamma$ , and  $\beta$  are related to the exchange interactions and magnetic anisotropy in the material [29],  $g$  is the gyromagnetic ratio, and  $k$  is a wavevector.

The calculated dispersion relations for  $\text{FeO}$  at 28 GPa with magnetoelastic coupling included [31] are shown in Fig.4a (estimated at  $T=295$  K), corresponding sound velocities are shown in Fig.4b. Dispersion relations (Fig.4a) change by less than 1 meV, well within the resolution of

neutron inelastic scattering experiment. However, as is evident from Fig.4b, the effect on the sound velocities is more pronounced, being almost 20-30 % within the energy transfer range up to 5 meV. This agrees reasonably well with the enhancement of the density of states which we observe in our experiment (Fig.3). Quantitative agreement may be sought along the lines of more elaborated theoretical models, similar to Ref. [34].

At present we do not have enough experimental information and theoretical understanding to better constrain the magnetoelastic coupling at  $T/T_N \sim 1$ . However, as follows from our observations, the effect is most pronounced close to the Néel transition. Our observations support the Mössbauer measurements, where the magnetic transition was observed starting from 8 GPa under nonhydrostatic conditions. The reason is that uniaxial strain along the body diagonal may induce magnetic moments well below the transition point determined under hydrostatic conditions (17 GPa). This is consistent with the notion that this second order phase transition is smeared by the external field (uniaxial strain), which is proportional to the order parameter of the broken symmetry phase [35].

In summary, we have observed substantial softening of the density of states at energy transfers below 10 meV in FeO at pressures close to 15-20 GPa, which persists in its antiferromagnetic phase up to 40-48 GPa. We relate the observed softening to the effect of the magnetoelastic coupling in this material. The theoretical estimates [25,22] show that both rhombohedral distortion and magnetoelastic coupling include substantial contributions from the magnetic anisotropy energy in FeO, which arises from the spin-orbit coupling in the orbitally degenerate ground state [24,25,27]. Further experimental work is required to clarify the effect of exchange-driven magnetoelastic contribution.

Portions of this work was performed at GSECARS, which is supported by the NSF, W.M. Keck Foundation and the USDA. The APS is supported by the DOE under Contract No. W-31-109-Eng-38. V. V. S. acknowledges Ron Cohen for bringing to his attention Ref. [27].

---

[1] H. K. Mao, J. Shu, Y. Fei, J. Hu, R. J. Hemley, Phys. Earth. Plan. Inter., **96**, 135 (1996).  
[2] H. K. Mao et al., Science **292**, 914-916 (2001).  
[3] M. Y. Hu, W. Sturhahn, T. S. Toellner, P. M. Hession, J. P. Sutter, and E. E. Alp, Nucl. Instr. and Meth. Phys. Res. A **428**, 551 (1999).  
[4] H. K. Mao, J. Xu and P. M. Bell, J. Geophys. Res. **91**, 4673 (1986).  
[5] G. Kugel, C. Carabatos, B. Hennion, B. Prevot, A. Revcolevshi and D. Tocchetti, Phys. Rev. B **16**,

378 (1977), G. Kugel, B. Hennion, C. Carabatos, in Proc. Symp. Neutron Inelastic Scattering, International Atomic Energy Agency, 1977, p.145.  
[6] T. Yagi, T. Suzuki, S. Akimoto, J. Geophys. Res. **90**, 8784 (1985).  
[7] Y. Fei and H. K. Mao, Science **266**, 1678 (1994).  
[8] R. Lübers, H. F. Grünsteudel, A. I. Chumakov, and G. Wortman, Science **287**, 1250 (2000).  
[9] Y. Sumino, M. Kumazawa, O. Nishizawa, W. Pluschkell, J. Phys. Earth, **28**, 475 (1980).  
[10] P. J. Eng, M. Newville, M. L. Rivers, and S. R. Sutton, in X-ray Microbeam Technology and Applications (Proc. SPIE-Int. Soc. Opt. Eng., 1998) p.145.  
[11] A substantial amount of work on the elastic anomalies at the Néel transitions was performed in 1960s [12]. 3d metal oxides exhibit extremely large anomalies in thermal expansion close to the Néel transition point [13], much larger than the corresponding anomalies for ferromagnetic materials [14].  
[12] H. S. Bennet, Phys. Rev. **185**, 801 (1969) and references therein, K. Kawasaki, I. Ikushima, Phys. Rev. B **1**, 3143 (1970).  
[13] M. Foex, Compt. Rend., **227**, 193 (1948).  
[14] K. P. Belov, *Magnetic Transitions*, Consultants Bureau, New York, 1961, 242 p.  
[15] C. G. Shull and J. S. Smart, Phys. Rev. **76**, 801 (1949); C. G. Shull, W. A. Strausser, and E. O. Wollan, Phys. Rev. **83**, 333 (1951).  
[16] Y.-Y. Li, Phys. Rev. **100**, 627 (1955).  
[17] W. L. Roth, Phys. Rev. **110**, 1333 (1958), ibid. **111**, 772 (1958).  
[18] B. Morosin, Phys. Rev. B **1**, 236 (1970).  
[19] D. Bloch and R. Maury, Phys. Rev. B. **7**, 4883 (1973).  
[20] G. Pepy, J. Phys. Chem. Solids, **35**, 433 (1974).  
[21] M. E. Lines and E. D. Jones, Phys. Rev. **139**, A1313 (1965).  
[22] L. C. Bartel, Phys. Rev. B. **1**, 1254 (1970).  
[23] D. Seino, J. of Mag. Mag. Mat., **28**, 55 (1982).  
[24] J. Kanamori, Progr. of Theor. Phys., **17**, 177 (1957).  
[25] J. Kanamori, Progr. of Theor. Phys., **17**, 197 (1957).  
[26] C. Kittel, Rev. Mod. Phys., **21**, 541 (1949).  
[27] I. V. Solovyev, A. I. Lichtenstein, K. Terakura, J. Magn. Magn. Mat. **185**, 118 (1998).  
[28] H. P. Rooksby and N. C. Tombs, Nature, **167**, 364 (1951).  
[29] S. V. Peletminskii, Sov. Phys. JETP, **37**, 321 (1960).  
[30] We have used Eq.12 from ref. [29] for zero external magnetic field, we neglect damping and eddy current contributions, and we use the relation  $\delta_1 - \delta_2 = B_2/2M_0^2$  for magnetoelastic constants (see Ref. [29] for  $\delta_1$  and  $\delta_2$  notation). Magnetoelastic waves are assumed to travel along the body diagonal of the cubic structure of FeO.  
[31] We estimated  $B_2 = -2.5 \cdot 10^{10}$  erg/cm<sup>3</sup> from the rhombohedral distortion using Eq.2;  $\rho = 6.2$  g/cm<sup>3</sup>, we assumed  $\gamma \ll \beta$ , and estimated  $\alpha = 10^{-6}$  erg·cm from P=0.1 MPa data [5].  $M_0 = 1400$  Gauss (mean field estimate for  $T/T_N = 0.85$ ,  $\mu_{eff} = 5.1 \mu_B$  [32]);  $\Omega = gM_0\beta = 2.6$  THz (11 meV) was estimated from Raman data [33].  
[32] A. Michel, P. Poix, J.-C. Bernier, Ann. Chim. **1970**, 265.  
[33] V. V. Struzhkin, A. F. Goncharov, N. Boctor, R. J. Hemley, H. K. Mao, Bull. Am. Phys. Soc. **46 II**, 812 (2001).

- [34] V. V. Gann, Sov. Phys. - Solid State, **9**, 2734 (1968).  
 [35] L. D. Landau and E. M. Lifshitz, Statistical Physics, Part I, Moscow, 1976.

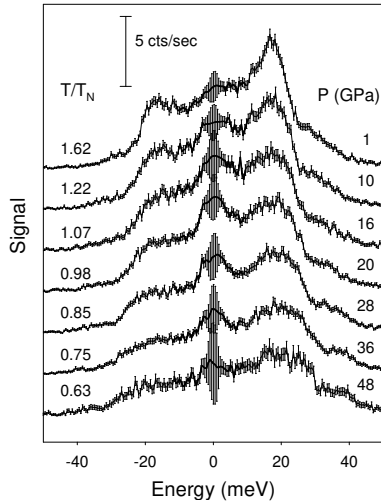


FIG. 1. Inelastic part of the signal in FeO as a function of pressure (elastic peak is subtracted). The region close to zero energy transfer is shown using bold lines. Note enhanced density of states close to  $T/T_N \sim 1$ . Ratio  $T/T_N$  was estimated using  $T_N=198$  K at  $P=0.1$  MPa, and data from Ref.[7].

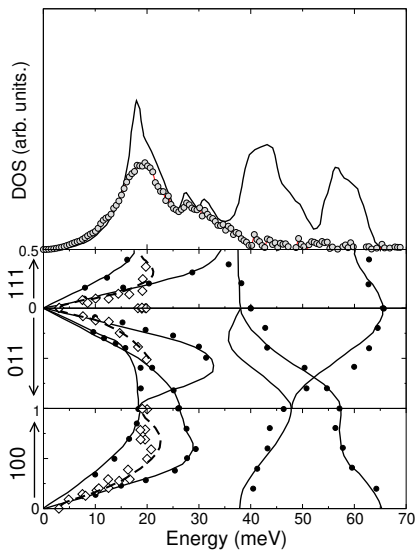


FIG. 2. Dispersion of phonons and magnons in FeO from neutron inelastic scattering experiments. Upper part shows comparison of phonon DOS calculated from neutron measurements (solid line) with our partial DOS for iron at 0.9 GPa (grey circles), 300 K. Also shown are measured and calculated phonon (circles and solid lines) and magnon (diamonds and dashed lines) branches from Ref.[5].

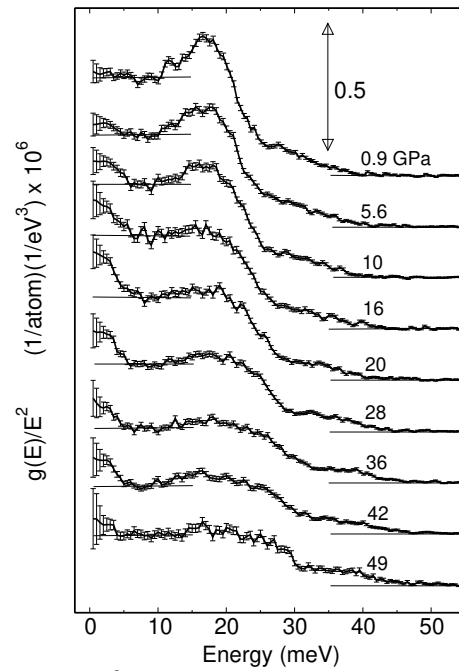


FIG. 3.  $g(E)/E^2$  derived from partial DOS in FeO as a function of pressure. For the Debye model, the lower energy part should be a horizontal straight line.

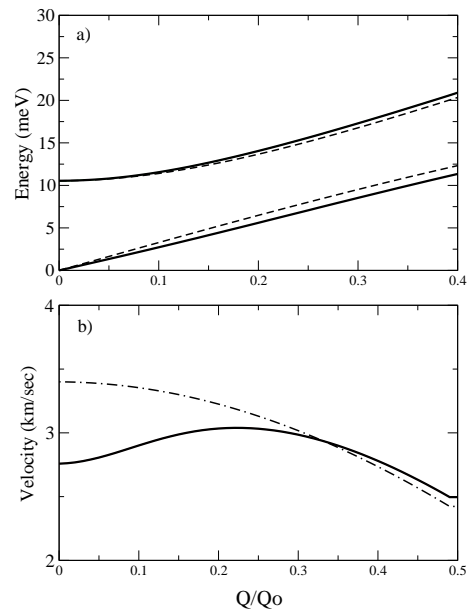


FIG. 4. Model for the magnetoelastic coupling in FeO. a) The interacting transverse phonon and magnon branches. Noninteracting bare frequencies are shown with dashed lines, the dispersion branch for magnons is calculated according to [31], the phonon dispersion was approximated by  $E(Q) = 2Q_0v_s/\pi \sin((\pi/2)(Q/Q_0))$  using the sound velocity 3.4 km/sec at  $Q=0$ . b) Calculated sound velocity including magnetoelastic coupling (solid line) and without magnetoelastic coupling (dash-dotted line).